Replies to referee comments (RC2)

RC2: 'Comment on egusphere-2024-1044', Johannes Hoppenbrock, 06 Jun 2024

The manuscript introduces marine Electrical Resistivity Tomography (ERT) as a technique for locating undersea permafrost. Using a relatively straightforward setup comprising 13 floating electrodes and an echosounder for determining water depths, multiple survey profiles around Tuktoyaktuk Island were measured. To mitigate corrupted ERT data, the cable was equipped with two GPS devices to monitor its curvature during the measurements. Various inversion methods were then tested and compared.

The manuscript demonstrates at which cable bending the geometry factor deviates significantly. These values are then filtered out. Additionally, a synthetic model was employed to investigate the impact of varying lateral and vertical smoothing constraints during the inversion process. Using the 'best-suited' inversion approach, the results indicate a slowly dipping permafrost table on the sea-facing northern side of Tuktoyaktuk Island and a more steeply dipping permafrost table on its southern side.

Overall, the manuscript is well written and easy to follow. However, to clarify the authors' approach further, a few structural adjustments could be beneficial (see general comments). When explaining the inversion process and its results, the authors could provide a more detailed introduction, analysis of the sensitivity and Depth of Investigation (DOI), as the results are primarily close to the resolution limits. Additionally, providing a brief overview of complementary methods and potential improvements to the inversion process at the end would help to properly contextualize the manuscript. These issues, along with several specific comments and technical corrections listed below, should be straightforward to address.

Thank you very much for these constructive comments. We address them below in detail.

General comments

Structure

Beginning the “Results” chapter, Chapter 3, with uncertainties might come across as somewhat pessimistic, and readers typically expect to encounter results immediately in this section. Perhaps Section 3.1 could be relocated to the analysis chapter, Section 2.3, or alternatively, to the end of Chapter 3.
Good point. (criticized by both reviewers). We will relocate Section 3.1 to the end of Chapter 3 in the revised version.

Additionally, Chapter 3.2, "Inversion and IBPT Depth," could be divided into two distinct parts: 1. Analysis and 'calibration' using synthetic data, and 2. Analysis of real data.
We agree that it is beneficial for the structure and have changed it as suggested.

Presentation of inversion results

Please provide additional information on how the inversion parameters, such as DOI and inversion RMS (e.g., in comparison to data residual), are determined. A sensitivity analysis

of e.g. the synthetic example would clarify how much the resistivity distribution at different depths can be expected to affect the measured data.
Thank you for your suggestion to add more details about the inversion process. Specifically, we provide i) a more detailed description of the calculation of the DOI (see comment on line 89), ii) an explanation of the data residual and how it compares to the RMS (see comment on line 200), iii) a brief overview of complementary methods and potential improvements to the inversion process (see 'Outlook and other Methods' below).

Including a figure that compares the synthetic model with the inversion result of the synthetic data would enhance the understanding of the synthetic study. Additionally, it would be beneficial to provide a second example of the real data inversion for comparison.
We didn't include these figures as we wanted to stick to not more than 5 figures, but we do see that they would be beneficial, so we included a figure that compares the synthetic model with the inversion result of the synthetic data and 5 additional examples of real data inversion in the Supplemental Online Material.

Outlook and other methods

Are there complementary methods/approaches to determine the depth of undersea permafrost? For an outlook the authors could also address possibilities to improve the inversion (e.g. 3D inversion or structural constraint inversion with different layers).
We have included complementary methods at the end of the discussion.
"In addition to marine ERT, other geophysical methods are able to detect permafrost depth in subaquatic environments (Angelopoulos et al. 2020). Reflection and refraction seismics have been widely used, especially in deeper areas (Brothers et al. 2012) but often demand higher logistical costs. An alternative and easily deployable method for shallow coastal areas relying on seismic signals has been presented by Overduin et al. (2015) who use ambient noise to detect subsea permafrost. Ground-penetrating radar can be effective in non-saline water areas for mapping frozen sediment, especially in bedfast ice zones (Stevens et al. 2009). Transient and controlled source electromagnetic surveys have also proven to be useful in offshore environments (Koshurnikov et al. 2016; Sherman and Constable 2018). Beside the presented inversion approaches, global ERT inversions have been shown to retrieve good results at estimating IBPT depths (Arboleda-Zapata et al. 2022). Identification of the IBPT independent of sediment and porewater characteristics, however, generally requires direct observation through drilling (Angelopoulos et al. 2020)."

Angelopoulos, M., Overduin, P. P., Miesner, F., Grigoriev, M. N., and Vasiliev, A. A.: Recent advances in the study of Arctic submarine permafrost, Permafrost Periglac., 31, 442–453, https://doi.org/10.1002/ppp.2061, 2020.

Brothers, L. L., Hart, P. E., and Ruppel, C. D.: Minimum distribution of subsea ice-bearing permafrost on the US Beaufort Sea continental shelf, Geophysical research letters, 39, 2012

Overduin, P. P., Haberland, C., Ryberg, T., Kneier, F., Jacobi, T., Grigoriev, M. N., and Ohrnberger, M.: Submarine permafrost depth from ambient seismic noise, Geophys. Res. Lett., 42, 7581–7588, https://doi.org/10.1002/2015gl065409, 2015.

Stevens, C. W., Moorman, B. J., Solomon, S. M., and Hugenholtz, C. H.: Mapping subsurface conditions within the near-shore zone of an Arctic delta using ground penetrating radar, Cold regions science and technology, 56, 30–38, 2009.

Koshurnikov, A., Tumskoy, V., Shakhova, N., Sergienko, V., Dudarev, O., Gunar, A. Y., Pushkarev, P. Y., Semiletov, I., and Koshurnikov, A.: The first ever application of electromagnetic sounding for mapping the submarine permafrost table on the Laptev Sea shelf, in: Doklady Earth Sciences, vol. 469, pp. 860–863, Springer, 2016.

Sherman, D. and Constable, S.: Permafrost Extent on the Alaskan Beaufort Shelf From Surface-Towed Controlled-Source Electromagnetic Surveys, J. Geophys. Res-Sol. Ea., 123, 7253–7265, https://doi.org/10.1029/2018JB015859, 2018.

Arboleda-Zapata, M., Angelopoulos, M., Overduin, P. P., Grosse, G., Jones, B. M., and Tronicke, J.: Exploring the capabilities of electrical resistivity tomography to study subsea permafrost, The Cryosphere, 16, 4423–4445, https://doi.org/10.5194/tc-16-4423-2022, 2022.

Specific comments

Line 2: comma after seawater: “Once inundated by seawater, permafrost usually begins to degrade.”
Corrected.

Line 11: Maybe more precise: “We discuss how marine ERT can be improved by accurately recording electrode positions, although choices made during data inversion are likely a greater source of uncertainty in the determination of the IBT position.”
Adapted.

Line 15: “permafrost degradation”
Corrected.

Line 39-40: Please give a reference for this prediction
We added Whalen et al. (2022).

Whalen, D., Forbes, D. L., Kostylev, V., Lim, M., Fraser, P., Nedimovíc, M. R., and Stuckey, S.: Mechanisms, volumetric assessment, and prognosis for rapid coastal erosion of Tuktoyaktuk Island, an important natural barrier for the harbour and community, Can. J. Earth Sci., https://doi.org/10.1139/cjes-2021-0101, 2022.

Line 42: “sea floor” or “seafloor”? Both is used in the manuscript.
We adopted the term “seafloor” throughout the paper.

Line 47: Are “frozen fresh water saturated sediments” equivalent to permafrost? Is there a sharp boundary between these two layers, or is it more of a transition?
Frozen fresh water saturated sediments is equivalent to permafrost formed before inundation. The transition can be expected to be relatively sharp due to the contrast in both state (frozen/unfrozen) and pore water resistivity (saline water/fresh water). We clarified this in the text the following:

"The method relies on the high resistivity contrast between frozen fresh water saturated sediment (i.e. former terrestrial permafrost) and unfrozen salt water saturated sediment (i.e. degraded permafrost) and uses a floating electrode cable dragged by a boat for current injection and voltage measurements."
For the sharpness of the boundary see comment RC1, line 207.

Line 48: "…a flexible cable in marine ERT survey relies on potentially varying electrode positions." -> "…a flexible cable in marine ERT survey results in potentially varying electrode positions. "
Adopted.

Line 49: Fig. 2 mentioned before Fig. 1
We removed the mention as figure 2 is referred to later in the text, when the survey design is introduced.

Line 55 / Figure 1: Figure appears before referenced in text
Corrected.

Line 60: "ice bonded" -> "ice-bonded"
Adopted

Line 60: "random massive ice bodies" -> "randomly distributed massive ice bodies"
Adopted.

Line 61: "On top of the cliff" -> "Above the cliff"
We changed the sentence to "The top of the island is mostly flat and covered by lowland and highland tundra with active layer depths around 60 cm."

Line 67: Please explain "thermoerosion"
We changed the sentence to: "Rising temperatures lead to an extension of the open water period, enhancing thermoerosion: the permafrost-cemented cliffs are exposed to heat transfer and mechanical abrasion from waves during a longer period of time, which accelerates permafrost thaw and thus coastal retreat (Berry et al., 2021)."

Berry, H. B., Whalen, D., and Lim, M.: Long-term ice-rich permafrost coast sensitivity to air temperatures and storm influence: lessons from Pullen Island, Northwest Territories, Canada, Arctic Science, 7, 723–745, https://doi.org/10.1139/as-2020-0003, 2021.

Line 68: Please introduce GSC
We added "Geophysical Survey of Canada (GSC)" with the first mention.

Line 86: Why reciprocal Wenner-Schlumberger array? Please discuss your choice concerning S/N ratio.
We added: "The reciprocal array has a lower signal-to-noise ratio because the minimum potential electrode separation is larger than the minimum potential electrode separation of the standard array. Furthermore, the reciprocal array is suitable for the survey design as it allows for simultaneous measurements during current injection."

Line 87: Why did you just use 13 of 22 electrodes? Maybe give a short explanation.
We changed the text to the following:

“The measurements were recorded with an IRIS Syscal Pro Deep Marine™ as a control unit, together with the IRIS software Sysmar™ on a connected field laptop. The IRIS Syscal Pro Deep Marine™ is designed to employ VES with 13 electrodes (2 injection electrodes and 11 potential electrodes, measured simultaneously on 10 channels). We used a custom-made cable with 22 electrodes (leaving 9 electrodes unused). This allowed for various electrode configurations and achieved greater penetration depth due to its increased length compared to the standard 13-electrode cable. In the electrode configuration used, the 13 electrodes combine to 10 roughly vertically stacked soundings with a quasi-common center but different pseudo-depths (Fig. 2).”

Line 89: You could include 'DOI' in brackets here to clarify the abbreviation for future references. Additionally, how was the DOI determined?
We changed “depth of investigation” to “pseudo-depth” as this term fits better here. The abbreviation DOI is introduced later.
The DOI was calculated during the inversion process in Aarhus Workbench, based on the approach of Vest Christiansen and Auken (2012) who provide an absolute measure for sensitivity. It is calculated based on the Jacobian matrix that is normalized with the standard deviation of the data points and the layer thickness. The sensitivity is then cumulated from the bottom upwards, where the empirically determined threshold of 0.75 is indicating the DOI.
We added an explanation for the calculation of the DOI later in the text (l. 130):
“The DOI was calculated internally during the inversion according to Vest Christiansen and Auken (2012) using a default sensitivity threshold of 0.75.”

Vest Christiansen, A. and Auken, E.: A global measure for depth of investigation, Geophysics, 77, WB171–WB177, https://doi.org/10.1190/geo2011-0393.1, 2012.

Line 93: “The water depth was measured from the boat for every sounding using an echosounder.” -> Please specify a bit more: Did you measure during the ERT measurement directly on the boat (velocity?)? In that case, there would be an offset of around 50 m to the point of maximum sensitivity and DOI of the ERT measurement.
The water depth was measured from the boat at a speed of around 7 km/h. The coordinates of the water depth measurements were recorded and later aligned with the coordinates of the center GPS coordinates. We made the following changes to the text:
“The GPS positions at the boat and at the center and tail of the cable were continuously recorded. The water depth was measured from the boat using an echosounder and later assigned to each sounding based on the coordinates of the cable center.”
And we added the boat speed in a previous sentence (l. 89):
“We used a floating multicore cable towed behind a boat at around 7 km/h to collect the soundings at a spacing of around 5 m.”

Line 104 / Figure 2: - What model was used to determine DOI? - Maybe add a depth scale and a label for the water body
See comment on line 89 for the determination of the DOI. We added a label for the water body, but we consider a depth scale not to be beneficial as it should be a schematic sketch.

Line 110: Figure 3a appears much later; perhaps show subpicture 3a) earlier
FInal figure layout will be set during typesetting.

Line 111: How was the geometric factor k calculated? Was the full problem solved (3D electrode positions) or only the variation of electrode distances?
The geometric factor was calculated assuming a homogeneous half-space (see Looke, 2001; eq. 1,9) and using the modified electrode positions (x and y coordinates) corresponding to a circularly bent cable for different degrees of curvature. For clarification, we added the following sentence to the manuscript: "…, the modified geometric factor k was calculated for every potential electrode pair (cf. Loke, 2001) ***considering the electrode positions and cable distortions in the horizontal plane."***

Loke, M.: Tutorial: 2-D and 3-D Electrical Imaging Surveys, https://www.researchgate.net/publication/264739285_Tutorial_2-D_and_3-D_Electrical_Imaging_Surveys, 2001

Line 117: Are the penalizing parameters of these four inversion types only applied to vertical resistivity contrasts or also to lateral resistivity contrasts?
Both. We added: "The different inversion types have different penalizing parameters regarding the minimization of the ***lateral and*** *vertical resistivity contrast between cells and thus result in models with different degrees of sharpness."*

Line 127: Why did you choose 10 Ohmm as the resistivity of the unfrozen sediment? Including a picture of the synthetic model could be generally helpful.
The threshold was chosen based on a paper from Overduin et al. (2012). The lab measurements in the paper showed that sediment with a resistivity of 10 Ohmm is almost certainly unfrozen, even in hypersaline environments. See Supplement below this document for a picture of the synthetic model.

Overduin, P. P., Westermann, S., Yoshikawa, K., Haberlau, T., Romanovsky, V., and Wetterich, S.: Geoelectric observations of the degradation of nearshore submarine permafrost at Barrow (Alaskan Beaufort Sea), J. Geophys. Res.-Earth, 117, https://doi.org/10.1029/2011jf002088, 2012.

Line 141: Please introduce RMS
Corrected.

Line 145: Please introduce GIS.
Corrected.

Line 168: Here, mainly Fig. 3c)
Corrected.

Line 169-171: Probably only a secondary effect, should be in the range of the error linked to 2D assumption as resistivity also depends on variation of resistivity perpendicular to the profile.
Yes, the effect is probably minor compared to the geometric factor variation (especially of an asymmetrically bent cable). The steepest parts of the estimated IBPT have a gradient of up to 0.35 m / m. At the maximum accepted distance difference of 1 m, the lateral deviation is around 6 m, which means, the IBPT can vary around 2 m in depth, which is a difference that can be resolved with ERT.

Line 177: “were removed” with d at the end
Corrected.

Line 177: “Soundings for which the difference varied were removed” What was the threshold here?
We added this information in the text:
“We applied a threshold of 125.7 m as a minimum distance between head and tail, which corresponds to the (mean) head-to-tail distance of the measurements with dd =1 m. For some profiles the head-to-tail distance was slightly lower but constant. For those profiles we tolerated soundings with a head-to-tail distance > 125.0 m.”

Line 185: When interpreting the data without additional information, whether the boundary layer lies above or below the DOI should not be an argument. Both are valid possibilities.
We agree that generally, both are valid possibilities and as we stated in line 268, we expect the DOI to be close to (below or above) the IBPT as the sensitivity drastically drops at the boundary to the frozen layer. However, for some models the inferred boundary lies tens of meters below the DOI where the sensitivity is so low that the resistivity distribution only has a negligible impact on the actual measurement and thus, the inversion outcome and the inferred boundary are very ambiguous. This aspect is also treated in Arboleda-Zapata et al. (2022) that we cite in the discussion.

Arboleda-Zapata, M., Angelopoulos, M., Overduin, P. P., Grosse, G., Jones, B. M., and Tronicke, J.: Exploring the capabilities of electrical resistivity tomography to study subsea permafrost, The Cryosphere, 16, 4423–4445, https://doi.org/10.5194/tc-16-4423-2022, 2022.

Line 195: Maybe not with cm accuracy here.
See comment RC1, l. 195+198.

Line 196: What is the grid cell size and what resolution could be expected according to the used electrode array in that depth?
The grid cell size and the resulting limit on resolution have been moved from the discussions to the results:
“At 20 m depth (approximate depth of the IBPT from 350 to 550 m offshore), the cell thickness is around 2 m, which leads to an even lower resolution at that depth and is also the reason for small but abrupt step-like changes in IBPT depth within only a few meters in the lateral direction. The uncertainties in IBPT depth due to inversion resolution thus range from ± 0.5 m to ± 1 m (half the layer thickness).”

Line 200: How is the data residual determined, and what is the difference compared to the inversion RMS?
The data residual is a metric used by the inversion software Aarhus Workbench:

$$data\ residual = \sqrt{\frac{1}{N}\sum_{i=1}^{N}\frac{(d_{obs,i} - d_{forward,i})^2}{(\sigma_{data,i} \cdot d_{obs,i})^2}}$$

where d_obs: observed data (resistivities),
d_forward: resistivities of the forward model,
σ_data: estimated noise level of the data (10%)
N: number of data points.

The data residual can be regarded as the RMS weighted with the standard deviation (noise level) of the measurement. If the data residual is close to 1, it means that the model is well-fitted and that the noise level of the model corresponds to the noise level of the data. A data residual < 1 suggests overfitting; > 1 underfitting. However, the used noise level σ_data is only a rough estimate, as we don't have repeated measurements to determine it more exactly (repeated measurements can be challenging with the applied survey design in a marine environment. Therefore, the data residual should be considered as an error estimate for comparison between different profiles, but not as an exact measure for underfitting or overfitting. The data residual and the RMS are calculated with the resistivity in linear space.

We added: "Goodness of fit between forward response and measured data was estimated using the data residual, a metric used by the inversion software Aarhus Workbench. It can be regarded as the RMS weighted with the standard deviation (noise level) of the measurement. A data residual close to 1 indicates a good fit between the resistivity and noise level of the model and data. As we only roughly estimated the noise level, the data residual should be considered as an error estimate for comparison between different profiles, but not as an exact measure for underfitting (data residual > 1) or overfitting (data residual < 1). The data residual and the RMS are calculated with the resistivity in linear space."

Line 204: Here you could split the chapter into "Synthetic model analysis" and "Real data analysis"
We agree that it would be beneficial and split the chapter as suggested.

Line 206: Was the water body a constraint in the inversion? Was there a variation in the CTD measurements or was it constantly 6 Ohmm?
The reference for the water layer resistivity was the CTD measurement closest to the profile of the CTD measurements taken on the same day as the ERT. The CTD profile selected was constantly at 6.1 +- 0.2 Ohm m.
We added the following statement to the methods section: "The water layer resistivity was set to a starting value 6.1+-0.2 Ohm m based on the CTD measurement closest to the profile and taken on the same day as the ERT and its variation constrained during inversion."

Line 235: Couldn't the movement of the cable also be determined by the history of the GPS data, allowing you to simulate the cable's movement?
Yes, that is correct. However, as we used only 3 GPS units, it was difficult to assess whether the cable curvature is perfectly circular or slightly asymmetric.

Line 254: To address this issue, you could potentially constrain the water layer within a range, e.g. between 5-6 Ohmm.
Varying the water resistivity during inversion tends to improve the fit between observation and inverted data. Since observations of water resistivity were relatively uniform, however, we did not feel that this was justified.

Line 269: Maybe you could provide this explanation earlier (see comment on line 185).
Our idea was to give this explanation in the discussion. But we could also briefly mention it in line 185.

Line 276: First 'or' in the sentence could be replaced with a comma.
Adopted.

Line 285: This is the resolution of the mesh. The capability to resolve resistivity contrasts of the inversion could be in a different range depending on your electrode configuration and resistivity distribution.
Yes, this is the resolution of the mesh. As the resolution of the measurements could allow a finer grid, in our case the grid is the limiting factor which makes it the overall resolution of our grid. But it would be interesting to assess the resolution of the measurement as you commented below.

Line 294: A finer grid does not necessarily improve the resolution of the measurement. An analysis of the sensitivity would be interesting to modify or adapt the electrode configuration in later studies.
A recent publication by Arboleda et al. (2022) studies the effect of electrode configurations on ERT survey accuracy and resolution. The sensitivity analysis indicated that electrode spacing significantly impacts survey reliability. The shortest quadripole was sensitive to both seawater and unfrozen sediments, while wider spacings enhanced sensitivity to deeper layers, particularly around inner electrodes. This highlights the importance of carefully selecting electrode spacing and configurations, especially in areas with significant resistivity variations. Proper adjustments can improve the detection and characterization of permafrost layers, optimizing data acquisition for various geological settings. We agree that further studies are required on this topic, especially the effect of changing the electrode array.

We have added the following sentence to the discussion section:
"....and optimizing the electrode array for detection and characterization of permafrost layers… (Arboleda et al., 2022)."

Arboleda-Zapata, M., Angelopoulos, M., Overduin, P. P., Grosse, G., Jones, B. M., and Tronicke, J.: Exploring the capabilities of electrical resistivity tomography to study subsea permafrost, The Cryosphere, 16, 4423–4445, https://doi.org/10.5194/tc-16-4423-2022, 2022.

Supplement

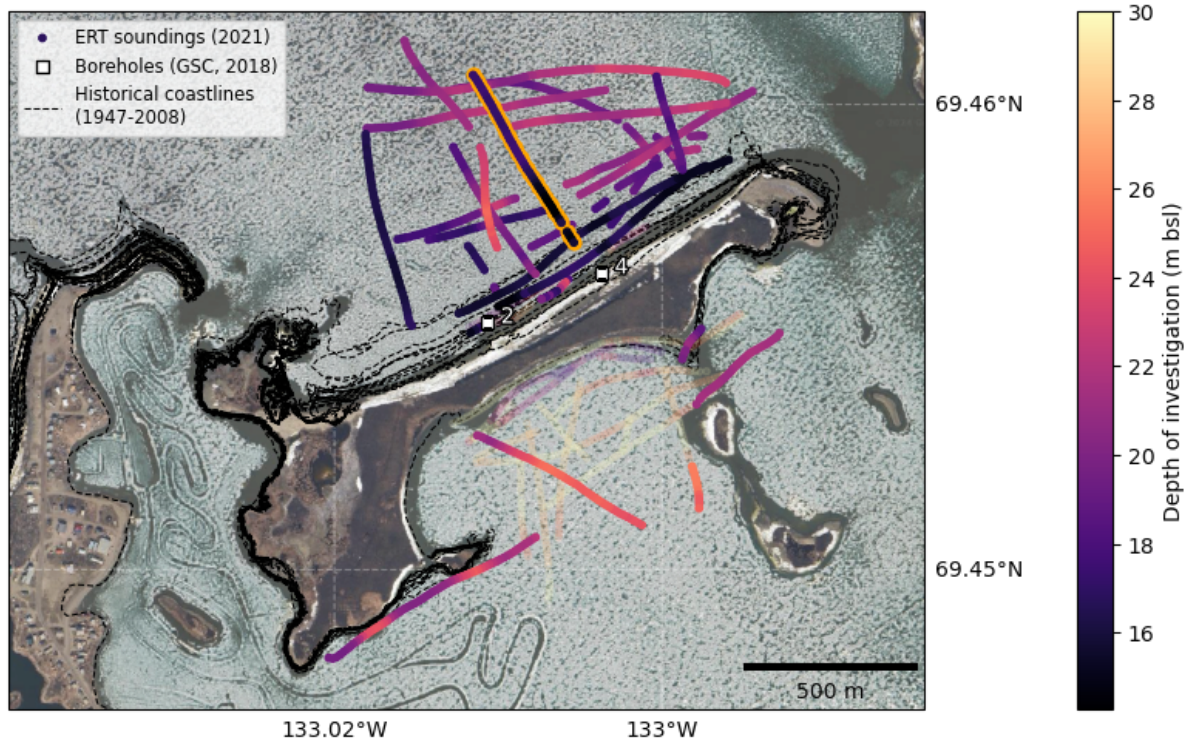

Supplement Figure 1: This figure shows a map of the ERT surveys conducted around Tuktoyaktuk Island (analogous to Fig. 5a). The survey lines are color-coded with the Depth of Investigation (DOI) in meters below sea level (m bsl). The DOI ranges from around 15 to almost 30 m bsl.

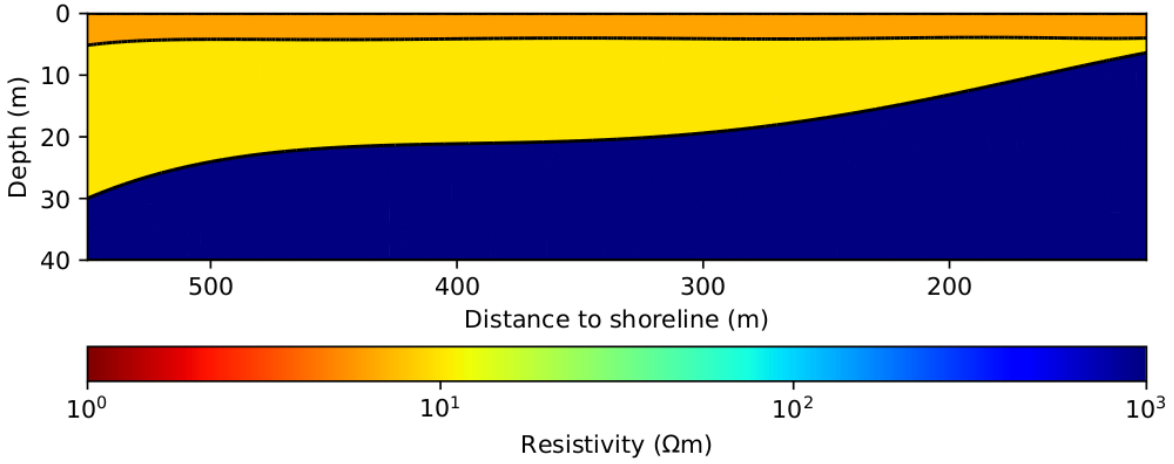

Supplement Figure 2: Synthetic model used to infer the most suited inversion technique for the specific setting. The model consists of 3 layers: The upper layer is representing the water body with a depth of 5 m and a resistivity of 6.1 Ohm m. The second and third layer have resistivities of 10 Ohm m and 1000 Ohm m, representing unfrozen and frozen sediment

respectively. The boundary between the two ranges between depths of 7 to 30 m and dips at varying angles, which is a plausible scenario for the IBPT in a profile perpendicular to the shoreline of Tuktoyaktuk Island.

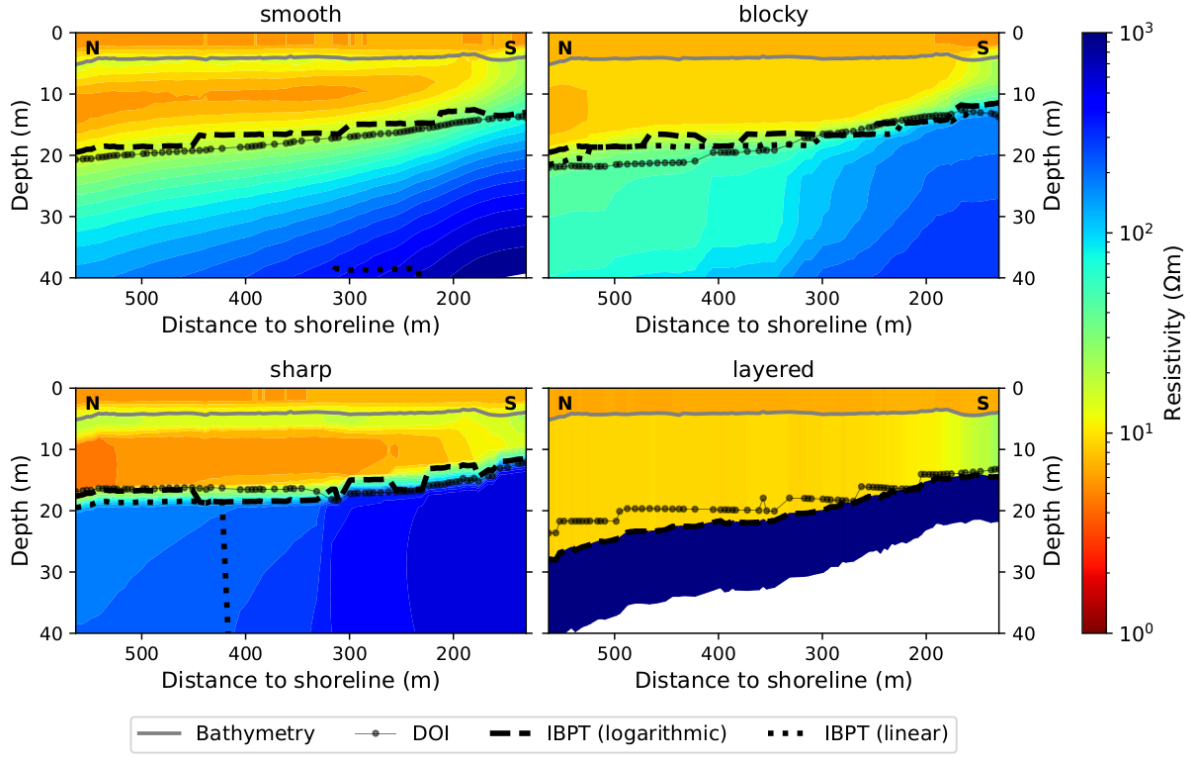

Supplement Figure 3: Comparison between the smooth, blocky, sharp and layered inversions of the synthetic model. The models show different transitions between the second and the third layer (unfrozen and frozen sediment in Supplement Fig. 2). The inferred IBPT as the highest vertical resistivity gradient in logarithmic space is close to the DOI in all four models. In the blocky model, the inferred IBPT is closest to the actual boundary in the synthetic model.

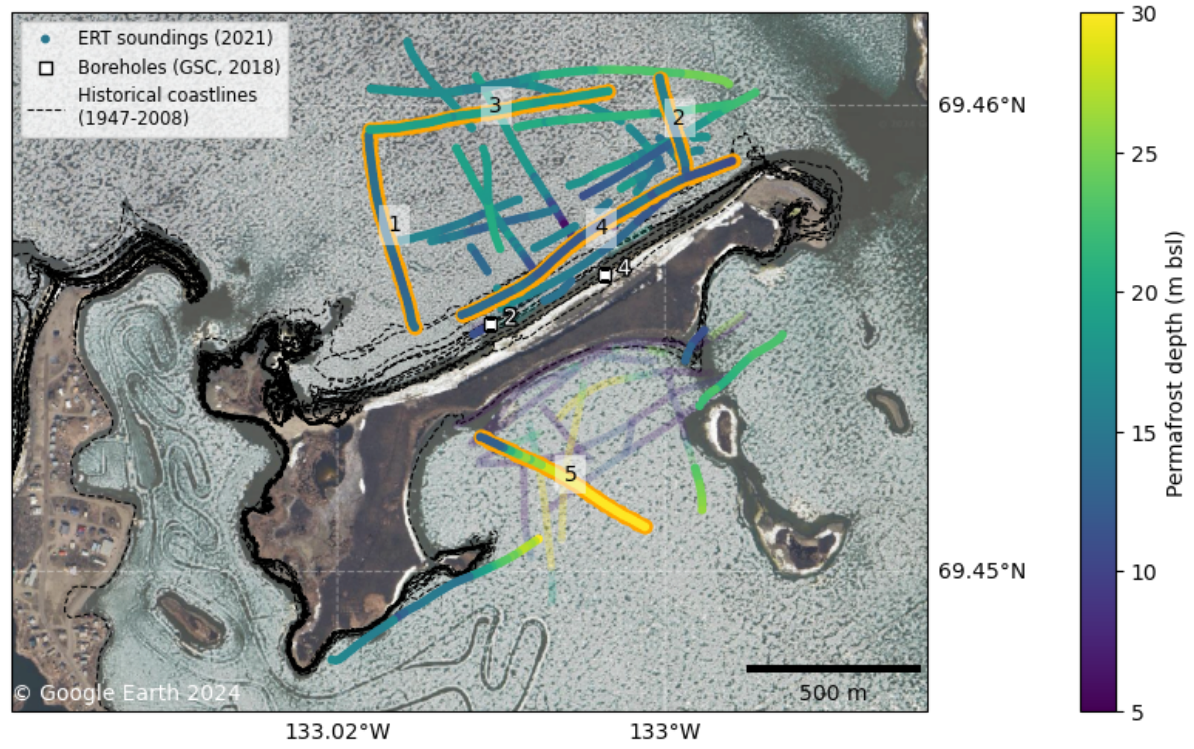

Supplement Figure 4: Overview map for supplemental profiles. The map shows all surveys conducted around Tuktoyaktuk Island and the inferred IBPT depth (as in Fig 5a). 5 profiles are highlighted that will be shown in the following.

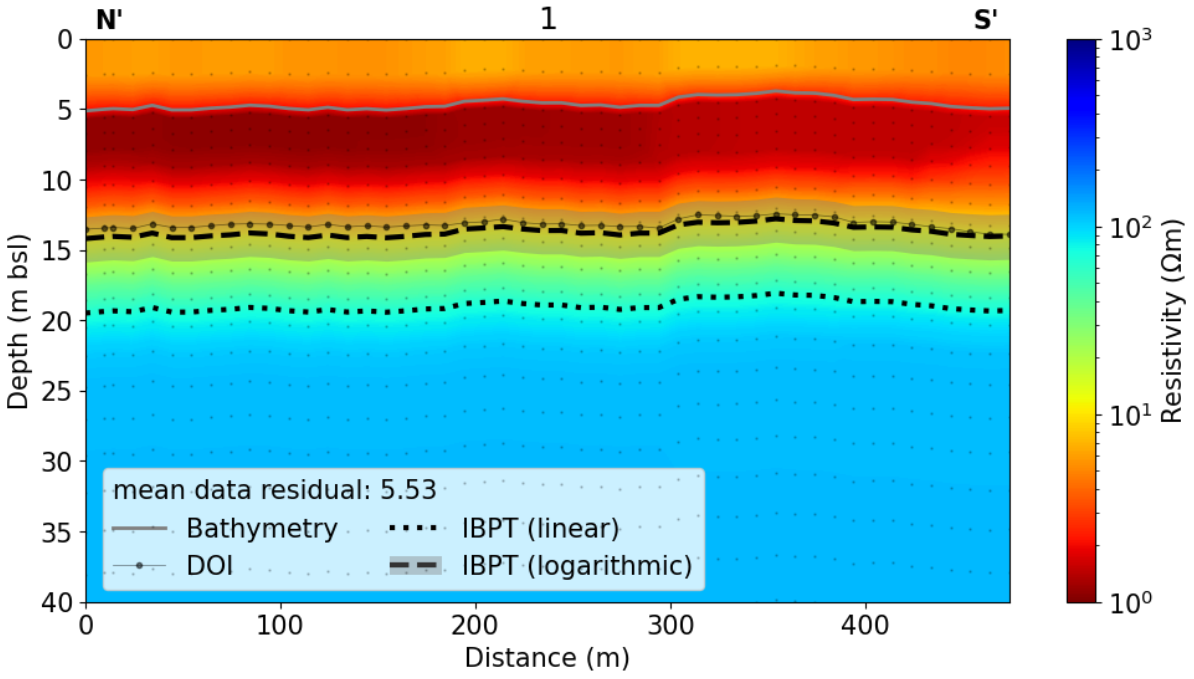

Supplement Figure 5: Inverted model of supplemental profile 1. The profile lies perpendicular to the northern shoreline and extends from North (offshore) to South (closer to the coast).

The water depth is around 5 m and the IBPT is inferred at around 14 m bsl, close to the DOI. Although the profile extends in North-South direction, and a dipping of the IBPT due to different inundation times along the profile is expected, the IBPT appears flat. However the fit of this inversion is rather poor, so the IBPT displayed here can be questioned.

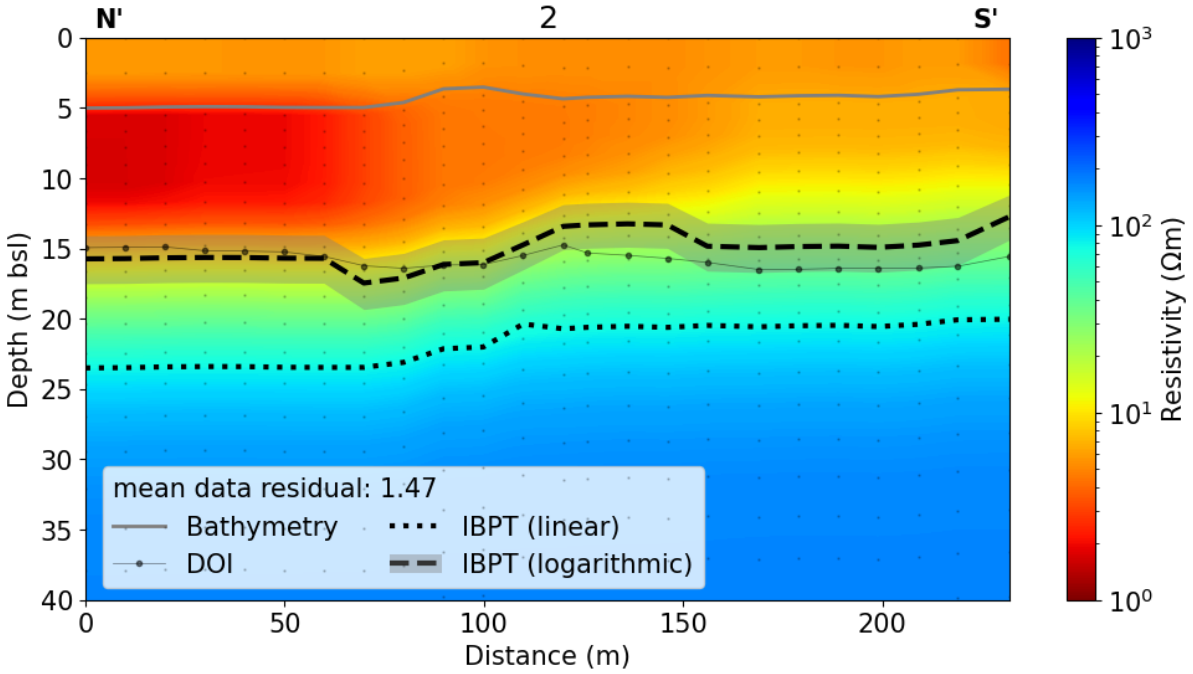

Supplement Figure 6: Inverted model of supplemental profile 2. The profile lies perpendicular to the northern shoreline and extends from North (offshore) to South (closer to the coast). The water depth is around 4 to 5 m and the IBPT is inferred at around 13 to 17 m bsl, close to the DOI. The dipping of the IBPT from South to North is not as pronounced as for the profile shown in Fig. 4 in the paper.

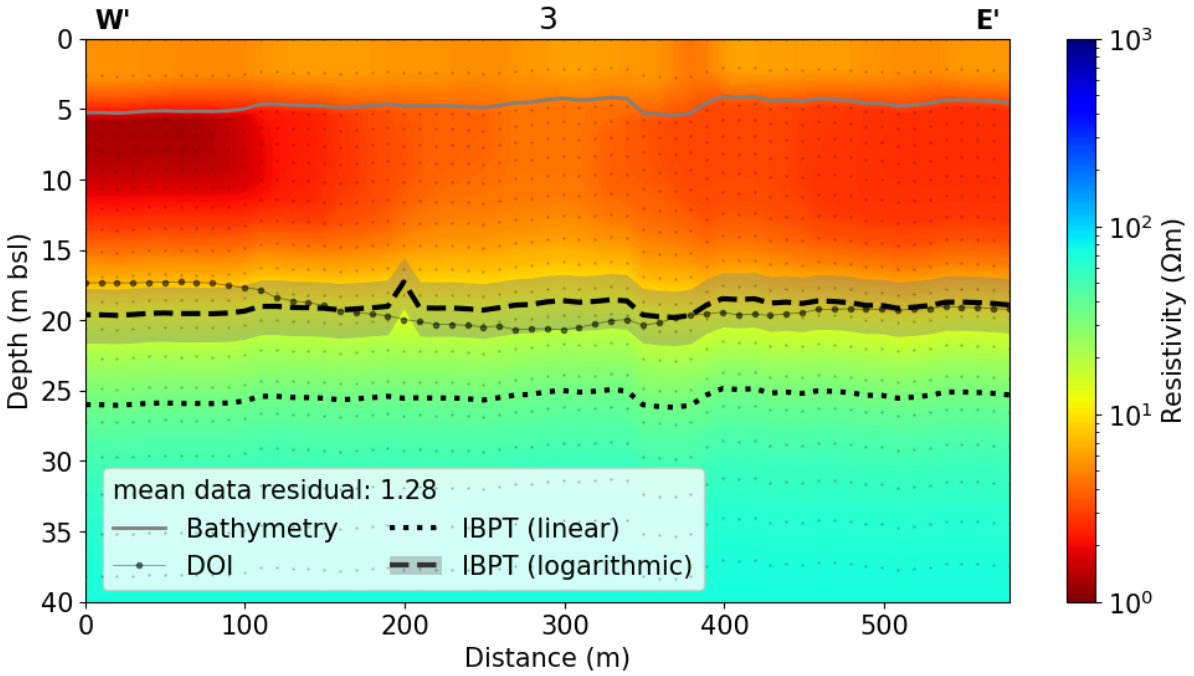

Supplement Figure 7: Inverted model of supplemental profile 3. The profile lies parallel to the northern shoreline and extends from West to East at around 500 to 700 m from the coast. The water depth is around 5 m and the IBPT is flat at around 20 m bsl, close to the DOI. Compared to profile 4 Supplement Fig. 8, the IBPT is more than 5 m deeper as profile 3 lies further offshore.

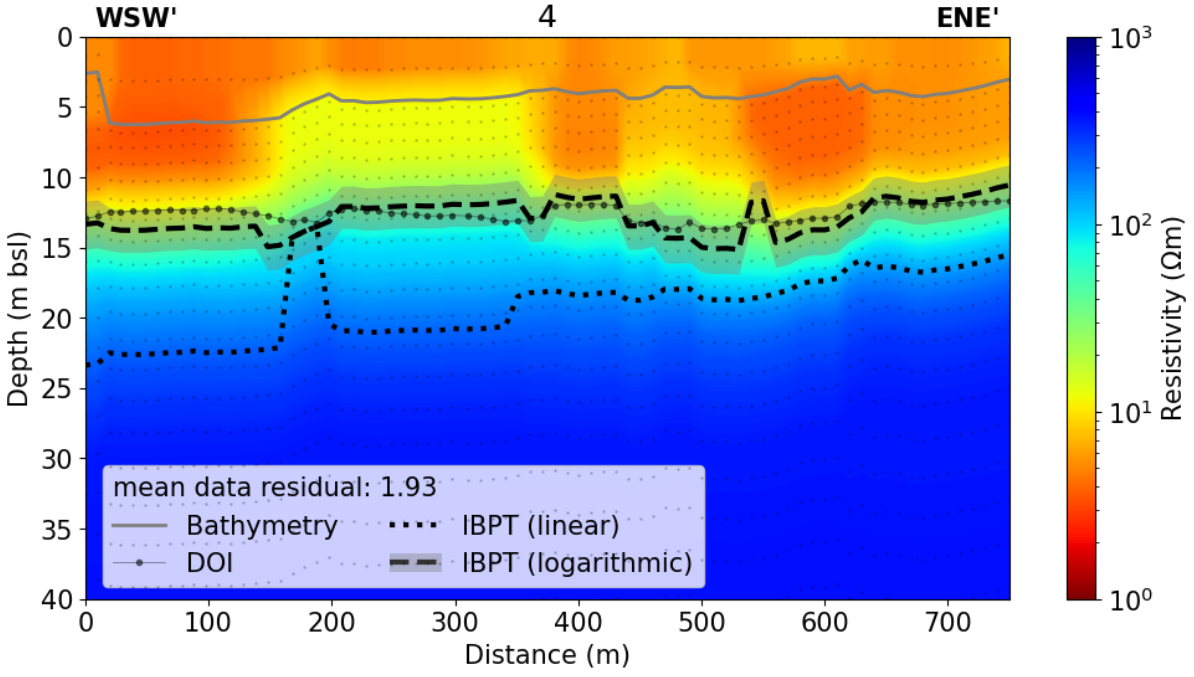

Supplement Figure 8: Inverted model of supplemental profile 4. The profile lies parallel to the northern shoreline and extends from (West-North-) West to (East-North-) East at around 150

m from the shore. The water depth is varying between 3 and 7 m and the IBPT is inferred between 12 and 16 m bsl, close to the DOI. Changes in Bathymetry and IBPT may appear more abrupt in comparison to the other profiles, as this is the longest profile and thus more compressed. The IBPT is shallower than in profile 3, as it lies closer towards the shore.

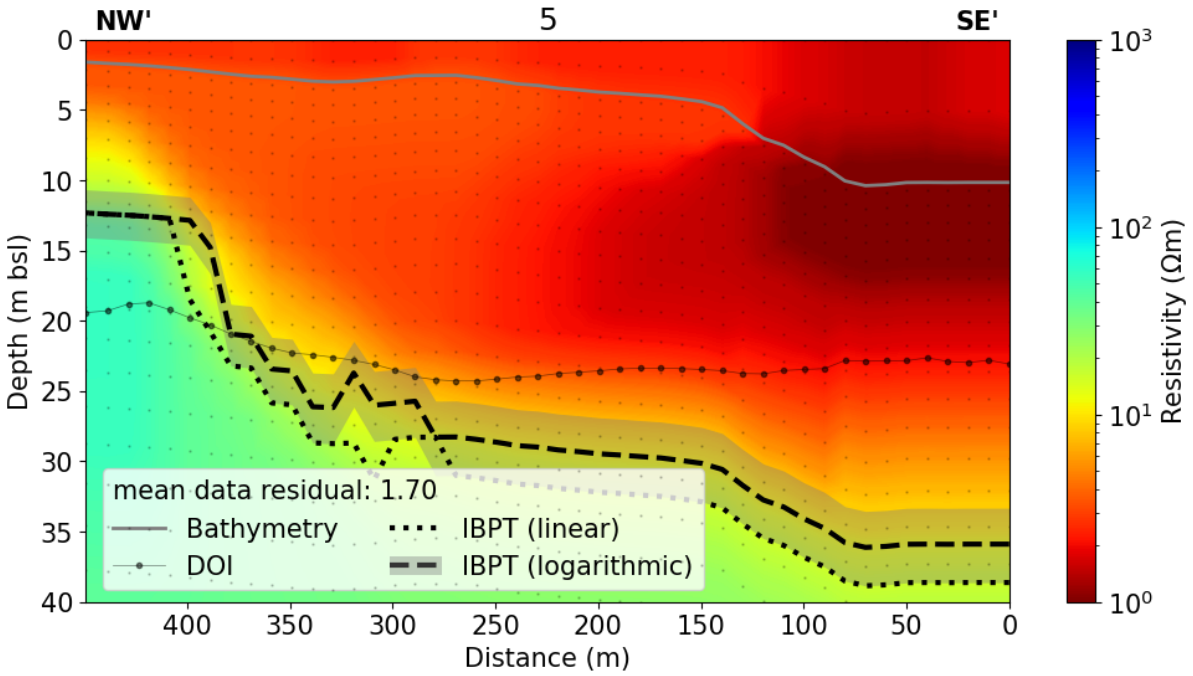

Supplement Figure 9: Inverted model of supplemental profile 5. The profile lies south of Tuktoyaktuk Island and extends from North-West (close to the coast) to South-East (towards the Harbor basin). The water depth ranges from 2 m close to the coast to around 10 m. The IBPT ranges from 12 m bsl close to the coast to around 35 m bsl where the water is deeper. A significant stretch of the IBPT lies several meters below the DOI, where the sensitivity is very low and the IBPT depth should be treated with caution. However we expect a deeper IBPT south of Tuktoyaktuk Island due to deeper water and slower coastal retreat rates that imply longer inundation times at similar distances from the coast and thus a longer period of subsea permafrost degradation.